Vol. 23, No. 3(2024) Alim24302
Revista Mexicana de Ingeniería Química

Evaluation of the particle size, water state, viscosity and viscoelastic properties (SAOS and LAOS) of yogurt samples with different protein contents (standard, protein-rich and high-protein Greek type)

Evaluación del tamaño de partícula, estado del agua, viscosidad y propiedades viscoelásticas (SAOS y LAOS) en muestras de yogurt con diferentes contenidos de proteína (estándar, rico en proteína y alto en proteína tipo Griego)

H. Espinosa-Andrews[1,2], J.N. Haro-González[1], J.A. Barbosa-Nuñez[1], E. Aguirre-Mandujano[2*], C. Lobato-Calleros[2]

[1] Unidad de Tecnología Alimentaria, Centro de Investigación y Asistencia en Tecnología y Diseño del Estado de Jalisco, A.C. Cam. Arenero 1227, El Bajío, 45019 Zapopan, Jal., México.

[2] Departamento de Preparatoria Agrícola y Posgrado en Ciencia y Tecnología Agroalimentaria, Universidad Autónoma Chapingo, km.38.5 Carretera México ? Texcoco, Texcoco, Edo. México 56230, México.

Received: March 28, 2024; Accepted: July 11, 2024

Abstract

The physical attributes of dairy products are related to the formulation, quality and processability of the product. In this work, the water state, particle size, viscosity, and viscoelastic properties of three yogurt formulations with different protein contents (standard, protein-rich and Greek-type) were evaluated. The melting enthalpy of water was evaluated by DSC, revealing that water molecules are found in different water states. Laser diffraction measured the particle size of the microgels; bimodal distributions were observed in the yogurts. The protein-rich and Greek-type yogurts had the smaller sizes with average D[4,3] values of 26.4 and 24.8 μm, respectively. The viscosity of the yogurts was fitted to the power law and Herschel-Buckley models, in which greater yield stress was found for the Greek-type yogurt. Small amplitude oscillatory shear experiments revealed the elastic behavior of the samples, with higher elastic moduli for the Greek-type yogurt. Large amplitude oscillation stress (LAOS) experiments were used to evaluate the nonlinear rheological response of the yogurts. 3D-Lissajous curves revealed that standard and high-protein yogurts display similar shear-thinning behavior as the shear stress increases, but this was less remarkable in the Greek-type yogurt. This study can be used to determine the most relevant parameters for dairy food formulation.

Keywords: yogurt, freezing water, particle size, viscosity, viscoelastic properties, Lissajous curves.

Resumen

Los atributos físicos de los productos lácteos están relacionados con la formulación, la calidad y la procesabilidad del producto. En este trabajo se evaluaron el estado del agua, el tamaño de partícula, la viscosidad y las propiedades viscoelásticas de tres formulaciones de yogur con diferentes contenidos proteicos (estándar, rico en proteínas y tipo griego). La entalpía de fusión del agua se evaluó mediante DSC, revelando que las moléculas de agua se encuentran en diferentes estados de agua. La difracción de Laser midió el tamaño de partícula de los microgeles; se observaron distribuciones bimodales en los yogures. Los yogures ricos en proteínas y de tipo griego tenían los tamaños más pequeños, con valores D[4,3] medios de 26,4 y 24,8 μm, respectivamente. La viscosidad de los yogures se ajustó a los modelos de ley de potencia y de Herschel-Buckley, en los que se encontró un mayor límite elástico para el yogur de tipo griego. Los experimentos de cizallamiento oscilatorio de pequeña amplitud revelaron el comportamiento elástico de las muestras, con mayores módulos elásticos para el yogur de tipo griego. Se utilizaron experimentos de tensión oscilatoria de gran amplitud (LAOS) para evaluar la respuesta reológica no lineal de los yogures. Las curvas 3D-Lissajous revelaron que los yogures estándar y ricos en proteínas muestran un comportamiento similar de adelgazamiento por cizallamiento a medida que aumenta la tensión de cizallamiento, pero esto fue menos notable en el yogur de tipo griego. Este estudio puede utilizarse para determinar los parámetros más relevantes para la formulación de alimentos lácteos.

Palabras clave: yogur, agua congelada, tamaño de partícula, viscosidad, propiedades viscoelásticas, curvas de Lissajous.

* *Corresponding author. E-mail*: eleagman@yahoo.com;
https://doi.org/10.24275/rmiq/Alim24302
ISSN:1665-2738, *issn-e*: 2395-8472

1 Introduction

Food processing has evolved over recent decades, and its main objective has been to preserve and stabilize food. Technologists are currently looking for improvements in sanitary and nutritional aspects, and textural and sensory attributes, and sustainable, safe and diverse production (Flores-Silva *et al*., 2022). Yogurt is a dairy product obtained by the fermentation of milk by *Streptococcus thermophilus* and *Lactobacillus delbrueckii* ssp. Bulgaricus, which produces lactic acid, which slowly decreases the pH of the system, creating a lovely protein gel (Sandoval-Castilla *et al*., 2004). The nutritional value of yogurt is usually greater than that of milk due to the higher content of protein, calcium, phosphorus, vitamins, and nutrients produced during fermentation (Vélez-Ruiz *et al*., 1997). Diverse types of yogurts are marketed around the world, e.g., standard yogurt, low-fat yogurt, Greek yogurt, vegan yogurt, and drinkable yogurt, among others, and their acceptance is often related to viscosity, texture, appearance, flavor, nutritional content, and mouthfeel (Farag *et al*., 2022). These characteristics are correlated with the composition of the sample (protein, fat, water, stabilizer agents, total solid content, etc), fermentation process conditions (temperature, starter cultures, fermentation reaction, etc), final pH, and physical properties of the final sample such as particle size distribution, viscosity, density, and water activity, among others (Erturk *et al*., 2021; Farag *et al*., 2022; Gilbert *et al*., 2021; Sala *et al*., 2008; Sandoval-Castilla *et al*., 2004). Dairy gels are recognized for their capacity to retain water, which is associated with proteins/carbohydrates to enhance the microstructure and quality of yogurts. DSC is one of the tools used to investigate water-related thermal processes, including crystallization, melting, protein denaturation, starch gelatinization and glass transition events (Espinosa-Andrews *et al*., 2018; Iijima *et al*., 2021). Water in foods has different thermodynamic states, including nonfreezing water (bounding water) and freezing water (which shows crystallization or melt transition during cooling or heating, respectively). In particular, the composition and fermentation process of yogurts can impact the water holding-capacity of the protein network altering the rheological properties and microstructure (Najgebauer-Lejko *et al*., 2020).

According to the literature, the microstructure of fermented dairy products such as fresh cheese and yogurt is described as a suspension of weakly interconnected microgels in a continuous phase (Gilbert and Turgeon 2020; Gilbert *et al*., 2021; Heck *et al*., 2021). Microgels are individual or aggregated fragments of primary particles of fat droplets and proteins (mainly whey protein/casein micelle complexes) that are not destroyed or partially destroyed during shearing (Moussier *et al*., 2019). The size and distribution of microgels depend on the formulation, yogurt formation process, storage conditions, and method of shearing. The size and distribution of microgels seem to partly explain the smoothness and creaminess of yogurts, but these properties are also related to the nature and rigidity of the microgels (Gilbert and Turgeon, 2021). Laser diffraction is a widely used material particle size measurement technique that offers fast measurements over a wide range of particles from 0.02 to 2000 μm with high repeatability, in which the particle size is measured indirectly by detecting intensity distributions of laser light scattered by particles at different angles. However, few studies have employed laser diffraction to measure the microgel size distribution because microgels present heterogenous three-dimensional structures, instead of spherical structures as proposed by the laser diffraction technique (Gilbert and Turgeon, 2021; Moussier *et al*., 2019). However, Gilber *et al*. (2020) used laser diffraction and optical microscopy techniques to compare the size distribution of high-fat and low-fat stirred yogurt; both techniques showed that yogurts contain microgels with monomodal distributions, where laser diffraction showed mean sizes approximately 10% smaller than those observed by optical microscopy, indicating that both techniques are suitable for characterizing yogurts.

Rheological measurements are employed to determine the viscosity, thixotropy, viscoelasticity, and structural properties of yogurt, characteristics related to the quality and type of ingredients, and manufacturing process (Divyang *et al*., 2016; Erturk *et al*., 2022). Typically, rotational experiments characterize the apparent viscosity, yield stress and thixotropy properties, while viscoelastic and structural properties are estimated by oscillatory or creep tests (Divyang *et al*., 2016; Audrey Gilbert *et al*., 2021). According to Martinez-Padilla (2024), structured foods that exhibit yield stress can also exhibit viscoelastic, shear-thinning and/or thixotropic behavior. Viscoelastic measurements are a way to test a material's solid-like (elastic modulus (G')) and liquid-like (viscous modulus (G")) responses simultaneously, typically determined within two regions known as the small amplitude oscillatory shear region (SAOS) and the large amplitude oscillatory shear region (LAOS) (Rogers, 2018). The most common rheological test is SAOS, in which the sample structure is measured by applying a low stress or strain amplitude sweep to avoid damage to the microstructure of the sample within the linear viscoelastic region (LVR). Yogurt is a predominantly elastic gel in the SAOS region that is mainly dependent on the microstructure of the protein-fat network and its affinity for water molecules (Erturk *et al*., 2021). The viscoelasticity of dairy foods relies on SAOS tests, but these tests provide little information on food mouthfeel, swallowing or processing (e.g., pumping and handling), where irreversible structural deformations occur. Ptaszek (2017) mentioned that large amplitude oscillatory shear (LAOS) tests combined with a high frequency are valuable measurements that can mimic industrial processing and oral processes during food consumption. For this instance, the LAOS experiments are obtained by applying oscillatory strains ($\gamma(\omega t) = \gamma_0 \sin(\omega t)$), which consequently impose a phase-shifted strain rate ($\dot{\gamma}(\omega t) = \gamma_0 \omega \cos(\omega t)$), to analyze the nonlinear rheological of the oscillatory shear stress $\sigma(t;\omega,\gamma_0)$ (Le *et al*., 2023). The rheological response of a material subjected to a sinusoidal input in the LAOS region is not always sinusoidal (Rogers, 2018). Most LAOS analyses in the literature are based on subjecting the material to a time sinusoidal strain; however, LAOS experiments can be measured using a strain-controlled rheometer or a stress-controlled rheometer with software that can simulate strain control, in which the sinusoidal shear stress ($\sigma(\omega t) = \sigma_0 \sin(\omega t)$) is input into a stress-controlled rheometer to measure the strain response (γ) or the geometric displacement (δ, rad) (Bae *et al*., 2013). As a consequence, the shear stress is also a time-varying signal $\sigma(t,\omega,\gamma)$ of the complex structure. The raw data can be extracted at each stress or strain applied, and a characteristic fingerprint of the microstructural changes can be plotted. Lissajous curves provide a graphical description of the nonlinear component, and they have been successfully used for the characterization of the rheological viscoelastic properties of doughs and viscous pectin solutions (Erturk *et al*., 2022), nixtamalized corn masa (Alvarez-Ramirez *et al*., 2019), yogurt oleogels (Aguilar-Zárate *et al*., 2019) and yogurts with different fat contents (Erturk *et al*., 2021). Thus, the evaluation of the physical and rheological characteristics of different yogurts is essential for the design of process equipment, new product development, quality control, and the development of sensory characteristics of the product. The objective of this work was to evaluate the water state, particle size, viscosity and viscoelastic properties of three yogurt formulations with different protein contents (standard, protein-rich and protein-high Greek type), with particular emphasis on the small- and large-amplitude oscillatory stress regions. This study will be helpful for evaluating yogurt properties because the rheological fingerprint is impacted by the water state, particle size and composition of the samples.

2 Materials and methods

2.1 Materials

Three yogurts were purchased from a local store in Zapopan (Jalisco, Mexico). Yogurt A (yA a high protein yogurt) contained: 5% protein, 6.9% carbohydrate, and 0% fat; yogurt B (yB a standard yogurt) contained: 3.4% protein, 12.5% carbohydrate, and 1.8% fat; and yogurt C (yC a high protein Greek-type yogurt) contained: 7.3% protein, 11.5% carbohydrate, and 2.3% fat.

2.2 Particle size distribution

The particle size distribution of the samples was measured via laser diffraction in a Mastersizer 3000+ (Malvern Instruments, Malvern, UK) following the method proposed by Gilbert *et al*.,(2020) with some modifications. Approximately, 0.1 g of yogurt was mixed with 400 ml of water at 1000 rpm for 5 min in a Hydro EV unit (Malvern Instruments). The particle size distribution was measured by means of five consecutive measurements after reaching an obscuration value between 14 and 16%. The particle size distribution was estimated, and the volume weighted mean (De Brouckere mean) was estimated D[4,3] using Mie's theory with refractive indices of water of 1.33 and 1.398 for the samples at 25 °C. Span is the width of the size distribution; the smaller the span values are, the narrower the distribution is. The span is calculated as:

$$Span = \frac{d(0.9) - d(0.1)}{d(0.5)} \tag{1}$$

The d(0.1), d(0.5) and d(0.9) are the sizes below 10%, 50% and 90% of the sample, respectively.

2.3 DSC measurements

The freezing water (W_f) state in the yogurts was estimated using differential scanning calorimetry (DSC 2000, TA-Instruments, New Castle, DE, USA). Tzero aluminum hermetic pans were used to load 15 mg of the samples. Each pan was mounted inside the DSC chamber, cooled to –40 °C and maintained isothermally for 5 min and then heated at 10 °C/min from –40 to 30 °C. An empty aluminum hermetic pan was used as a reference. Nitrogen at 50 mL/min was used to purge the instrument. Indium and deionized water standards were used to calibrate the DSC temperature. Two measurements were made per sample. Universal Analysis 2000 software (version 4.7a, TA Instruments) was used to estimate the melting temperature (T_m) and melting enthalpy (ΔH_m) of the samples. The percentage of freezing water (W_f) was calculated by

$$W_f(\%) = (\Delta H_m / \Delta H_w) \times 100\% \quad (2)$$

where ΔH_w is the melting enthalpy of pure water (334 J/g) (Iijima *et al*., 2021). The peak deconvolution procedure was carried out considering that the experimental melting peak contains two Gaussian curves estimated by the Peakfind subroutine of the OriginPro 2024 software (free version, Origin laboratories).

2.4 Rheological measurements

Rheological measurements were performed using a stress control rheometer (AR1000, TA Instruments; Newcastle, DE, USA) equipped with a Peltier system for temperature control at 5 °C. A crosshatched plate-plate geometry with a diameter of 40 mm diameter and a truncation gap of 1000 μm was used. The viscosity of the samples was calculated by a steady-state procedure. The samples were subjected to a preshear deformation of 10 s^{-1} for 2 min to establish an equal loading history. An equilibrium time of 5 min after pre-shearing was established for all samples to allow the recovery, which was verified with a time sweep test (data not shown). The viscosity of the sample was then measured using the steady-state flow procedure, in which a shear rate ramp from 0.1 to 100 s^{-1} was used. The sample period was every 10 s, considering a percentage of tolerance between measurements less than 5% in three consecutive measurements within tolerance. If this condition was not achieved in 90 s, then the software reported the data collected in the last 10 s.

The power and Herschel-Bulkley models were used to fit the shear properties of the yogurts. In the power model, η is the viscosity (Pa·s), n is the power law constant (dimensionless), and k is the flow consistency index (Pa·s).

$$\eta = k\dot{\gamma}^{n-1} \quad (3)$$

In the Herschel-Bulkley model, σ is the shear stress (Pa), σ_0 is the yield stress (Pa), K is the consistency index (Pa·s^n), and n is the behavior index (dimensionless).

$$\sigma = \sigma_0 + K\dot{\gamma}^n \quad (4)$$

The steady shear models of the yogurts were fitted using the software Rheology Advantage Data Analysis (TA Instruments).

Rheological oscillatory tests were performed based on the procedure proposed by Ortíz-Deleón *et al*. (2023) with some modifications. Stress sweeps were applied from 1 to 1000 Pa at two oscillation frequencies (6.28 rad s^{-1} and 62.8 rad s^{-1}). All the experiments were performed in triplicate. The LVR or SAOS region was estimated by the rheometer software. The frequency sweep curves were obtained from 0.628 rad s^{-1} to 62.8 s^{-1} within the SAOS region, and the storage modulus (G'), loss modulus (G'') and $tan(\delta)$ were recorded and reported.

The structural behavior of yogurts produced in the SAOS and LAOS regions was analyzed using Lissajous curves by plotting the stress vs strain and stress rate vs strain. Additionally, the SAOS and LAOS responses were visualized in a 3D space with osc. stress, osc. stress rate and osc. strains as coordinate axes. The Lissajous-Bowditch loops were used for detailed information on the structure of yogurt that was not obtained in the LVR.

2.5 Statistical analysis

One-way analysis of variance (ANOVA) was performed using Statgraphics Centurion XV 15.2.06 statistical software (StatPoint Technologies, Inc., Warrenton, VA, USA). Tukey's test was performed to identify significant differences among treatments ($p < 0.05$).

3 Results and discussion

3.1 DSC analysis

DSC is an important tool that can be used to evaluate the water state in food products (Rodríguez-Rodríguez *et al*., (2019). Depending on the interaction of water with the food matrix, water molecules can be found as freezable or nonfreezable water. Figure 1 shows the DSC thermograms of yogurts from -40 to 30 °C, in which the melting enthalpy of freezing water (ΔH_m) in yogurts is shown. In general, all yogurt samples showed one endothermic transition peak associated with the melting enthalpy of water. The melting enthalpies and melting temperatures estimated for the yogurts are shown in Table 1. Water in foods has different thermodynamic states, including nonfreezing water and freezing water. The first does not display any thermal signals because water is strongly bonded to compounds such as proteins, carbohydrates, fibers, etc. The other is freezing water, which can freeze, resulting in crystallization when it cools or melts when it heats. Freezing water can be found as free water and freeze-bound water. Free water does not interact with the macromolecules of the samples, exhibiting the typical properties of pure water (i.e., a melting point close to 0 °C), but may contain ions that may slightly alter the melting temperature. Freezing-bound water consists of water molecules weakly associated with proteins, starches or other molecules, has a lower melting point than free water and is typically associated with the quality of foods. The percentage of freezing water is related to the chemical composition of the samples but also to the affinity of the macromolecules for binding water and was estimated to be 63.2% 44.3% and 45.1% for yA, yB and yC, respectively. As expected, the yC sample displayed a low freezing water percentage, but surprisingly yB showed a similar value, probably related with the carbohydrate content that could have been added as a viscosity enhancer. According to Rodríguez-Rodríguez *et al.* (2019), the melting transition of freezing water is composed by the sum of the melting enthalpy of free water molecules and the melting enthalpy of freezing bound water over the temperature range. To investigate the state of water in different yogurt samples, the melting enthalpy of water was deconvoluted into two different Gaussian peaks (Figure 1). We propose that the peak that corresponds to a melting temperature closer to 0 °C is associated with the free water, and that the other peak corresponds to freezing-bound water. By applying a deconvolution procedure, it was found that the melting peak of yogurts is well described by two endothermic peaks with R^2-adjusted values of approximately 0.9977 for yA, 0.9907 for yB and 0.9974 for yC. The first peak was associated with freezing bound water with peak temperatures of -3.9, -2.8 °C and 2.4 °C and the estimated areas were approximately 53.1% for yA, 69.9% for yB and 33.2% for yC. The presence of freezing bound water is related to water bound to proteins, starches, and other components of the formula. The second peak was associated with the free water in the samples with peak temperatures of -1.9, -1.6 °C, and 0.1 °C. For samples yA and yB, this temperature was slightly different from that of pure water because small molecules such as salts, ions, or sugars in the sample depreciate the melting point. However, this behavior was not observed in the yC sample due to the Greek yogurt draining process, during which minority compounds such as lactic acid and mono- and disaccharides were removed.

3.2 *Viscosity of yogurts*

The rheological characteristics of yogurt are impacted by the solid content, stabilizer content, milk source, milk composition, starter probiotic composition, heat treatment, pumping conditions, manufacturing conditions and storage conditions (Suwannasang *et al.*, 2022). Figure 2a shows the viscosity curve of the samples at 5 °C. It is well known that yogurts exhibit shear thinning behavior when aggregate particles become disordered as they progressively move as a result of a high shear rate range (10^{-3} to 1000 s^{-1}) (McClements, 2023). However, the experimental viscosity of the yogurts did not display a plateau at low shear rates (< 0.1 s^{-1}), probably because the experimental conditions used were not low enough to observe this region. Based on these results, the samples exhibited a non-Newtonian behavior, which was adjusted to different rheological models (Table 1).

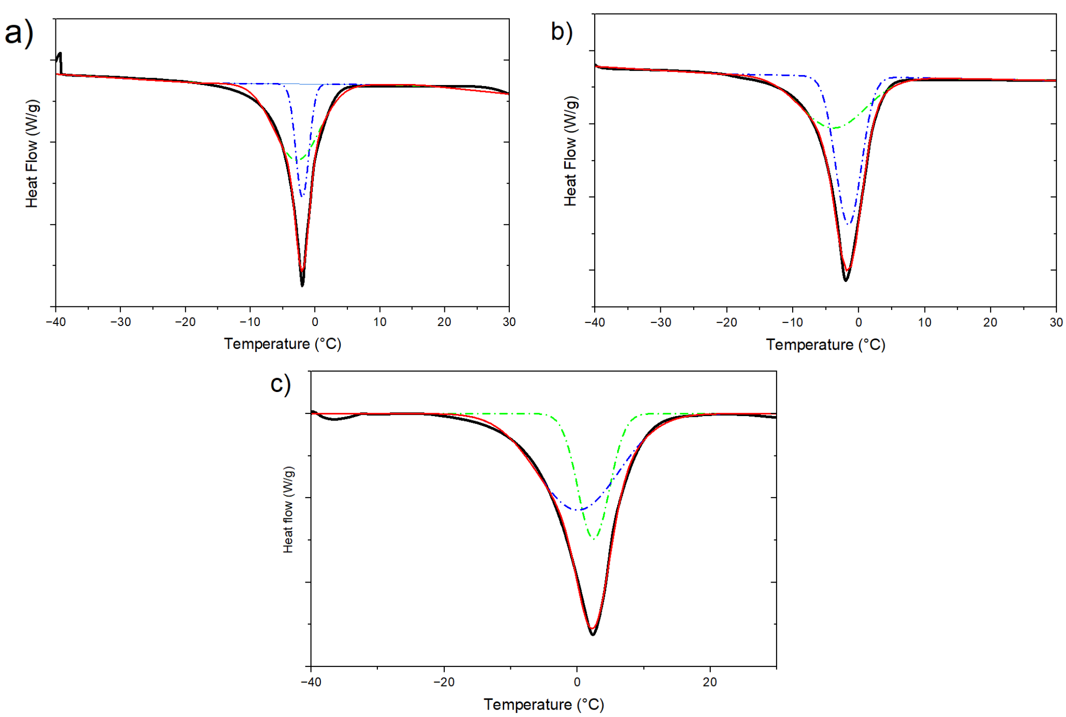

Figure 1. DSC thermograms of the yogurt samples: a) yA, b) yB, and c) yC. The experimental data (black solid line), cumulative fitted curve (red solid line), freezing bound water (dashed green line) and free water (blue dashed line) are shown.

Table 1 Thermal, rheological and size properties of the yogurts.

Sample		Units	yA	yB	yC
Melting enthalpy		(J/g)	211.1 ± 8[a]	148.0 ± 5[a]	150.4 ± 2[a]
Melting temperature		(°C)	-2.7 ± 0.1[a]	-1.9 ± 0.1[b]	-2.4 ± 0.1[c]
Freezing water		(%)	63.2[a]	44.3[b]	45.1[b]
Power law					
$\eta = k\dot{\gamma}^{\mathbf{n-1}}$	k	Pa·s	27.13	22.67	99.43
	n	dimensionless	0.0029	0.0354	0.0622
	R^2		0.9841	0.9956	0.9986
Herschel-Bulkley model					
$\sigma = \sigma_0 + K\dot{\gamma}^{\mathbf{n}}$	σ_0	Pa	17.65	16.55	55.83
	K	Pa.s^n	17.79	9.374	49.38
	n	dimensionless	0.2563	0.3516	0.1925
	R^2		0.9142	0.9781	0.9863
D [4,3]		(μm)	26.4 ± 1.3[a]	33.9 ± 0.2[b]	24.8 ± 1.1[a]
Span		-	1.94 ± 0.10[a]	2.04 ± 0.05[a]	3.62 ± 0.27[b]

[a & b] Different letters in the same column represent significant differences between treatments.

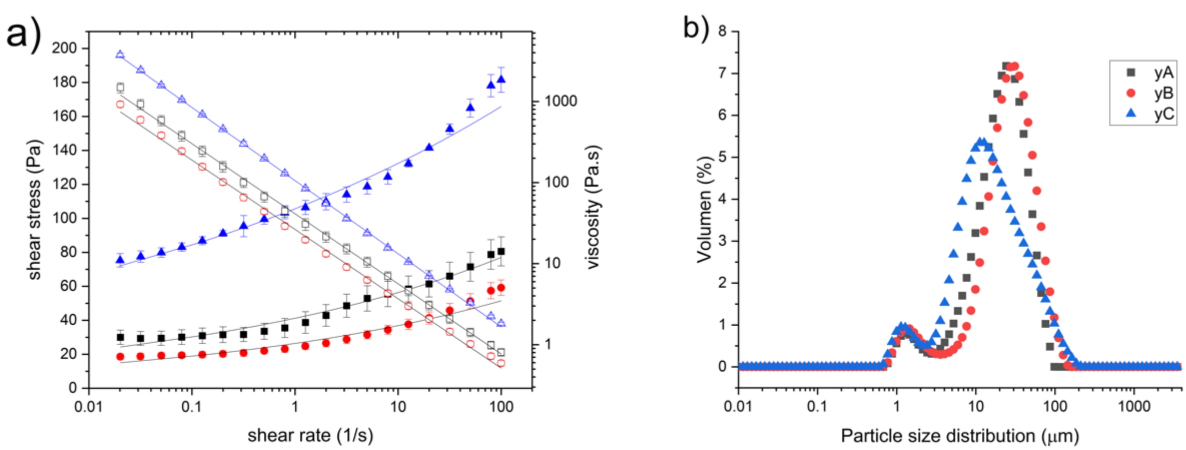

Figure 2. a) Viscosity curves of yogurt samples. Viscosity (open symbols) and shear stress (close symbols). b) Particle size distribution of the yogurt samples. Symbols: yA (squares), yB (circles) and yC (triangles).

The power law was used to describe the viscosity behavior of the samples and the Herschel-Bulkley model was used to calculate the yield stress of the sample, which is the minimum shear stress required to start to flow (Martínez-Padilla, 2024). The yield stress of the samples followed the order: yC (55.83 Pa) > yA (17.65 Pa) > yB (16.55 Pa), a value associated with the microstructure of the samples.

3.3 *Particle size of yogurts*

Figure 2b shows the particle size distribution of the samples. All the size distributions obtained by laser diffraction were bimodal, with a small peak at approximately 1.2 μm and a second peak in the interval from 2.5 to 100 μm. Table 1 describes the mean particle size distribution of the microgels, in which samples with high protein content (yA and yC) showed significant differences from sample yB. According to these results, yC displayed a lower particle size distribution and the highest span number of the samples, indicating that the presence of particles is associated with the protein network. Similar results were presented for sample yA to those presented by Moussier *et al.*(2019), who reported the size distributions of a commercial low-fat yogurt (0.1% fat and 4.5% protein) using laser diffraction, observing a monomodal particle distribution with a D[4,3] of 25.4 ± 0.4 μm and a span value of 1.6 ± 0.04. According to Gilbert and Turgeon (2021), as the shear stress increases, the size of the yogurt network decreases, reducing the viscosity.

3.4 *Viscoelastic properties*

The stress sweeps curves of yogurt at different oscillation frequencies are shown in Figs. 3a and 3b.

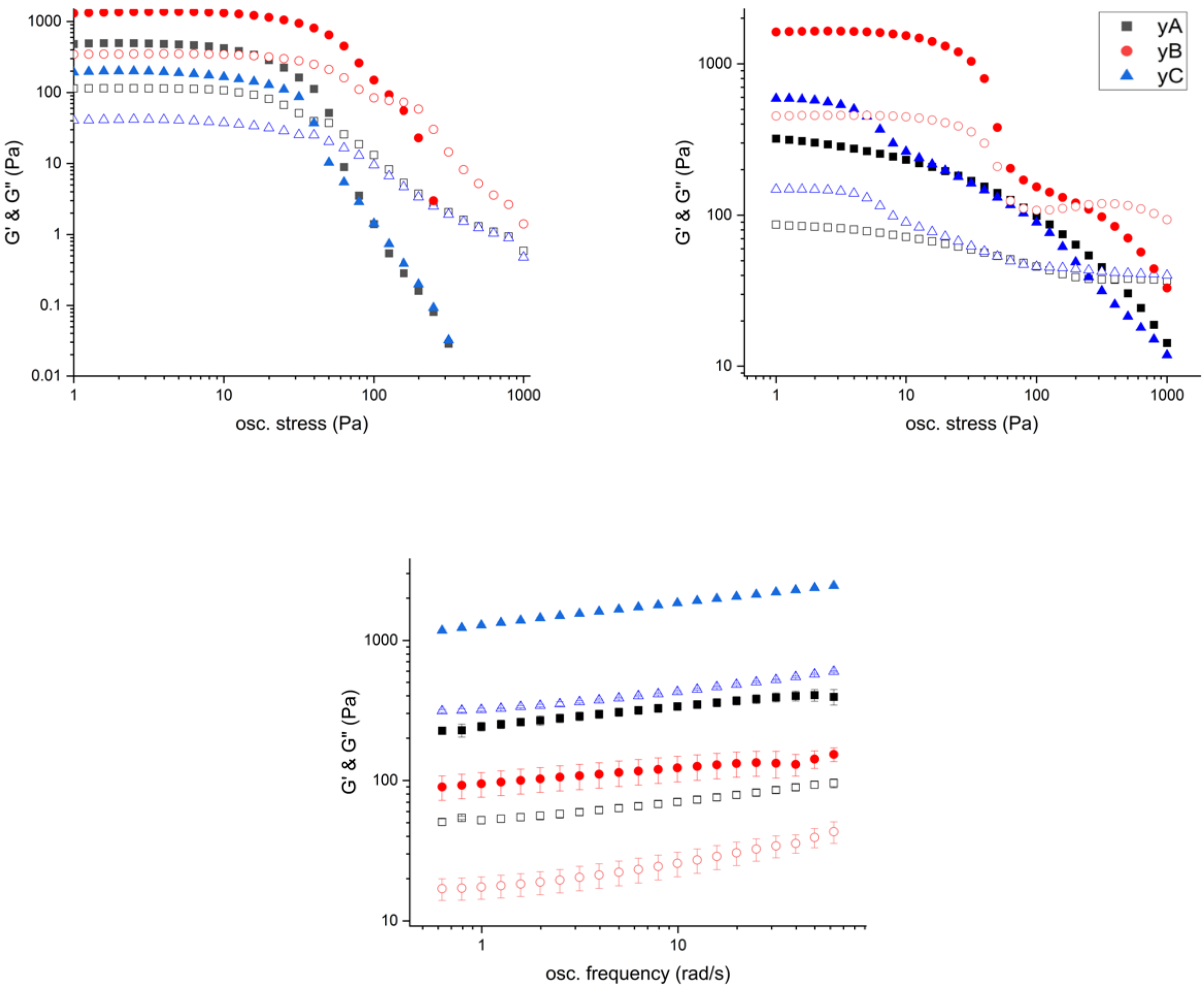

Figure 3. Stress curves of yA (squares), yB (circles) and yC (triangles) at 5 °C. a) 6.28 rad s^{-1}, b) 62.8 rad s^{-1}, and c) frequency sweeps of yogurts at 5 °C and 6.28 rad s^{-1}. G' (close symbols) and G" (open symbols).

The viscoelasticity of the yogurts depends on the applied oscillation stress and frequency, displaying two typical rheological regions, the SAOS and LAOS regions. The SAOS region can be located in the region where the rheological moduli do not change significantly (typically less than 5%) and is commonly reported as the lineal viscoelastic region (LVR). The yield point of the samples was measured by taking the onset point of the elastic moduli and finding the LVR at applied stresses lower than 10 Pa for samples yA and yB and below than 25 Pa for sample yC (Fig. 3a). The elastic modulus predominated over the viscous modulus in the SAOS region. It was observed that yC had a greater rheological modulus and LVR at a constant frequency than the other samples due to its higher protein content (7.3%) and fat content (2.3%), which produced a more structured viscoelastic matrix. In the SAOS region, sample yA had an elastic modulus more than twice that of yB but three times lower than that of sample yC at a given frequency; i.e., at an oscillatory stress of 5 Pa and 6.28 rad/s, the G' of yA (476 Pa) was higher than that of yB (189 Pa) but almost three times lower than that of yC (1389 Pa).

The damping factor, *tan(δ)= G"/G'*, expresses the relative contribution of the viscous and elastic parts to the viscoelastic response (Li *et al*., 2021). The *tan(δ)* values in the LVR for samples yA, yB and yC were estimated in 0.21, 0.29 and 0.27, respectively. Typically, the *tan(δ)* value is lower for more structured materials, reaching values of 0.01 for true gels. Chakraborty *et al*. (2018) reported that *tan(δ)* values between 0.2 and 0.3 indicate the typical amorphous polymeric behavior of yogurt samples. However, as the applied stress increases to the LVR of the samples, the G' and G" values decrease, revealing the crossover point of the rheological moduli, known as the sol-gel point (*tan(δ)=1*). This point increased with the increasing applied frequency from 6.28 to 62.8 rad s^{-1}, with values ranging from 43.3 Pa to 223 Pa for sample yA; from 34 Pa to 395 Pa for sample yB; and from 138 Pa to 220 Pa for sample yC. At low frequency (6.28 rad s^{-1}), the change in G' is more abrupt showing a steeper slope for samples yA and yB than for yC. At high frequency (Figure 3b), all samples show overshoot in

G", a behavior reported for structured foods, such as mayonnaise by Le and coworkers (2023), who related this behavior to unrecoverable deformation and creep. Finally, it is worth noting the presence of a small valley in the loss modulus values measured at low frequency in the LAOS region, induced by particle jamming that opposes alignment along the direction of the oscillatory flow (Crispín-Isidro *et al*., 2015; Hyun *et al*., 2011).

Figure 3c shows the oscillation frequency sweep curves of the yogurt samples in the SAOS region at 5 °C. Typically, this curve shows the viscoelastic behavior of yogurts without being subjected to deformations within the nonlinear region. The elastic modulus predominates over the viscous modulus for all the samples, with a slight dependence on the oscillation frequency. The highest elastic moduli were presented by sample yC, demonstrating a greater degree of structuring of the sample at low frequencies, in which the *tan(δ)* values ranged between 0.18 and 0.25 (equivalent to phase angle (*δ*) values between 10.2 and 17.6°). Erturk *et al*., (2021) reported that phase angle values increase as the yogurt structure breaks down and becomes more fluid and reported in oscillatory frequency experiments within the RLV that the delta value for yogurts with different fat contents ranging from 22 to 36° was significantly greater than that reported in our work.

3.5 Lissajous-Bowditch curves

Elastic Lissajous-Bowditch curves describe the instantaneous intracycle behavior of a material subjected to an oscillatory stress at a given oscillatory frequency and temperature, providing information on microstructural transitions of the material as it moves from the SAOS region to the LAOS region (Li *et al*., 2021). Fig. 4 shows the normalized Lissajous curves of yogurts (yA, yB and yC) evaluated at different stresses (1, 2.5, 5, 10, 25, 40, 50, 80, 100, 250, 500, and 1000 Pa) at 6.28 rad s^{-1} and 5 °C.

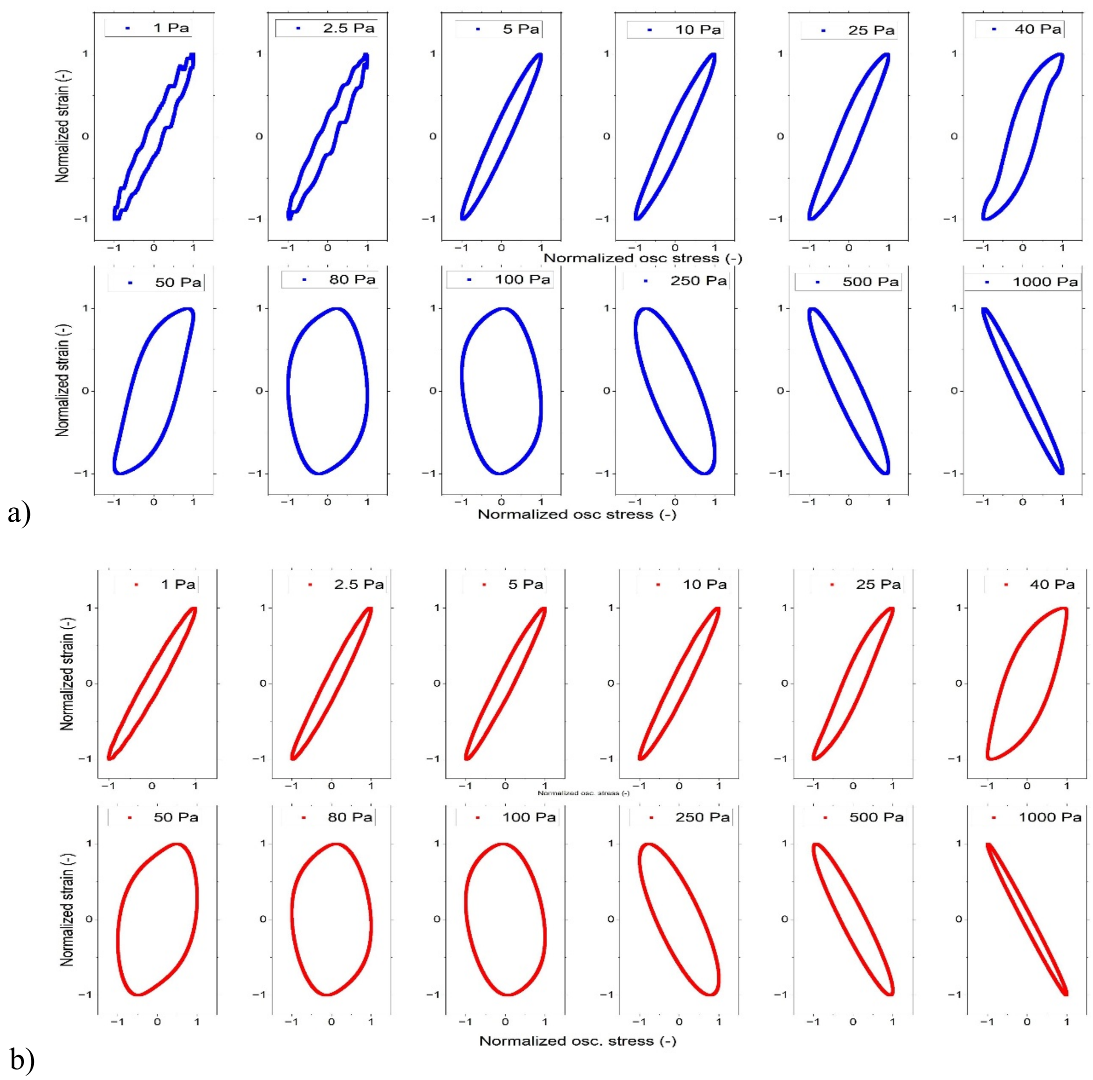

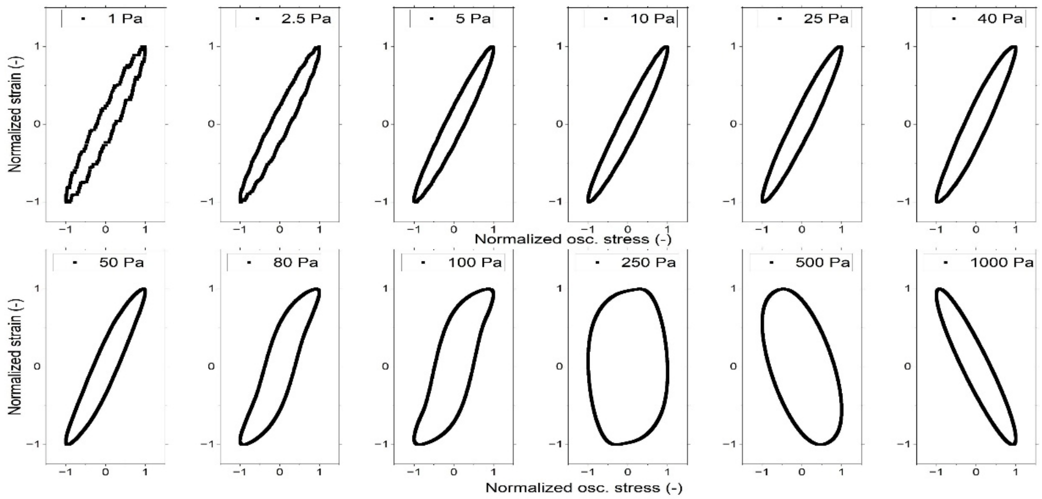

c)

Figure 4. Normalized Lissajous plots of yogurts at 6.28 rad s^{-1} and 5 ºC: a) yA, b) yB and c) yC. All intracycle data were normalized to the maximum stress or strain in the oscillatory cycle.

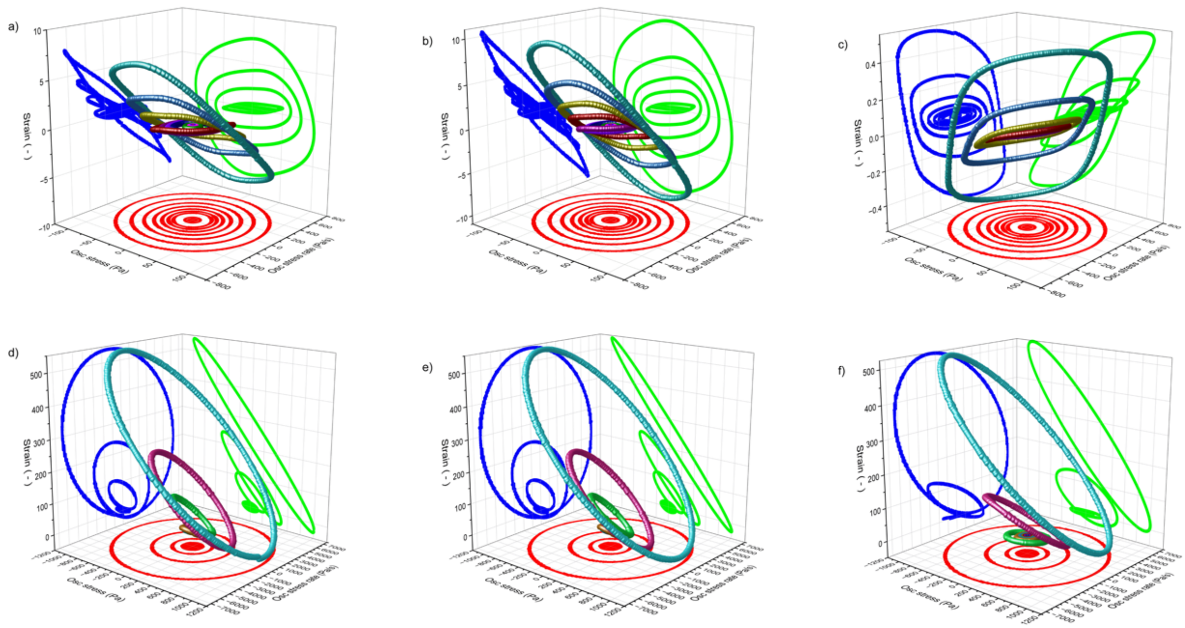

Figure 5. 3D Lissajous plots of yogurts with varying oscillatory stress at a constant frequency of 6.28 rad s^{-1} and 5 °C: yA (a) and (d), yB (b) and (e), and yC (c) and (f). The oscillatory stress varies from 1 to 600 Pa in figures a-c and from 600 to 1000 Pa in figures d-f. Projection curves displaying the elastic component (green), and viscous component (blue) versus osc. stress and osc. stress rate, respectively.

Similar to what was found in this work, Erturk *et al*., (2021) reported that the area of each normalized loop increased progressively at higher stresses, indicating that the amount of energy lost in each cycle was due to changes in the microstructure of the sample. In the LVR regime, the values of the rheological moduli are independent of the applied oscillation stress, and the oscillatory strain response is sinusoidal and shows a similar response with an elliptical behavior in the normalized Lissajous curves, which is typical of a solid-viscoelastic structure. With increasing stress in the range of 25 to 100 Pa, elliptical shape distortions were observed, and these distortions were greater in samples yA and yB. Erturk *et al*. (2021) observed for yogurt samples with different fat contents that the elastic elliptical projections of yogurt in the linear region progressively transformed into distorted parallelograms, indicating a shift from linear elastic behavior to predominantly viscous contributions in the nonlinear region. The elliptical shape distortion of Lissajous curves is related to the different microstructural characteristics and structural responses of materials subjected to large deformations (Ptaszek, 2017).

Figure 5 shows the 3D-Lissajous plots (unnormalized) of yogurt extracted from the oscillatory stress applied from 1 Pa to 1000 Pa at a constant frequency of 6.28 rad s^{-1} and 5 °C. Below an oscillation stress of 600 Pa (Figure 5a, 5b, and 5c), the distortions of the Lissajous curve are greater for sample yB than for samples yA and yC due to greater changes in its microstructure, probably because sample yB had the lowest protein and fat content, and the highest mean particle size, which increases its susceptibility to shear changes. That is, the applied oscillation stress can weaken, alter or disrupt intramolecular protein-protein, protein-lipid and protein-starch interactions, so these interactions are more likely to break during large deformations, resulting in a greater change in the nonlinear response. Instead, sample yC showed slight changes in the applied oscillation stress due to the high degree of structuring. These results are related to the greater oral sensation of the sample compared to that of the other samples. Finally, figures 5d-f show the 3D Lissajous curves when high oscillation stress is applied, in which the loss of microstructures is evident for all the samples.

Conclusions

The yogurt properties are impacted by their composition (protein content, fat content and water content). DSC is a tool that provides information on the proportions of free water and freezable bound water in yogurt, which are interrelated with the microstructure of the samples. The large particle sizes were linked with a low viscosity. The viscosity of the yogurt samples fit well to the power law and Hershel-Buckley models, showing that the viscosity and yield stress of the samples were dependent on the protein content, particle size and water state. A small amplitude oscillation shear experiment showed that the elastic nature of the yogurts was related to the protein network, while a large amplitude oscillation stress experiment allowed the evaluation of the microstructural changes in the yogurts in the nonlinear viscoelastic regime. The rheological characteristics of yogurts are vital tools that can support the development and quality of dairy products, as they provide a fingerprint of food behavior.

Acknowledgements

The first author is grateful to CIATEJ for the permission granted to carry out the sabbatical stay and to CONAHCYT for the grant awarded in the call for National Sabbatical Stays 2023-1, #852573.

References

Bae, J.-E., Lee, M., Cho, K. S., Seo, K. H., & Kang, D.-G. (2013). Comparison of stress-controlled and strain-controlled rheometers for large amplitude oscillatory shear. *Rheologica Acta*, *52*(10–12), 841–857. doi: https://doi.org/10.1007/s00397-013-0720-8

Chakraborty, P., G Rudra, S., Vishwakarma, R., Shivhare, U., Basu, S., & Chavan, R. (2018). *Rheological and Textural Properties of Milk Gels* (pp. 259–292). doi: https://doi.org/10.1201/9781315169408-11

Crispín-Isidro, G., Lobato-Calleros, C., Espinosa-Andrews, H., Alvarez-Ramirez, J., & Vernon-Carter, E. J. (2015). Effect of inulin and agave fructans addition on the rheological, microstructural and sensory properties of reduced-fat stirred yogurt. *LWT - Food Science and Technology*, *62*(1), 438–444. doi: https://doi.org/10.1016/j.lwt.2014.06.042

Divyang, M., Prajapati, Shrigod, N., Prajapati, Er. R., & Pandit, P. (2016). Textural and Rheological Properties of Yoghurt: A Review. *Advances in Life Sciences*, *5*, 5238–5254.

Erturk, M. Y., Bonilla, J. C., & Kokini, J. (2021). Relationship of non-linear rheological properties and quantitative network analysis parameters as a function of increasingly large amplitude deformations in non-fat, low-fat and high-fat yogurt products. *Food Hydrocolloids*, *111*, 106194. doi: https://doi.org/10.1016/j.foodhyd.2020.106194

Erturk, M. Y., Rogers, S. A., & Kokini, J. (2022). Comparison of Sequence of Physical Processes (SPP) and Fourier Transform Coupled with Chebyshev Polynomials (FTC) methods to Interpret Large Amplitude Oscillatory Shear (LAOS) Response of Viscoelastic Doughs and Viscous Pectin Solution. *Food Hydrocolloids*, *128*, 107558. doi: https://doi.org/10.1016/j.foodhyd.2022.107558

Espinosa-Andrews, H., & Rodríguez-Rodríguez, R. (2018). Water state diagram and thermal properties of fructans powders. *Journal of Thermal Analysis and Calorimetry*, *132*(1), 197–204. doi: https://doi.org/10.1007/s10973-017-6868-1

Farag, M. A., Saleh, H. A., El Ahmady, S., & Elmassry, M. M. (2022). Dissecting Yogurt: the Impact of Milk Types, Probiotics, and Selected Additives on Yogurt Quality. *Food Reviews International*, *38*(sup1), 634–650. doi: https://doi.org/10.1080/87559129.2021.1877301

Flores-Silva, P., Martínez-Yañez, R. C., Rodríguez-Huezo, M. E., & Alvarez-Ramirez, J. (2022). Nutritional protein quality and digestibility changes during food processing. *Revista Mexicana de Ingeniería Química*, *21*(1), 1–30. doi: https://doi.org/10.24275/rmiq/Alim2748

Gilbert, A., Rioux, L.-E., St-Gelais, D., & Turgeon, S. L. (2020). Studying stirred yogurt microstructure using optical microscopy: How smoothing temperature and storage time affect microgel size related to syneresis. *Journal of Dairy Science*, *103*(3), 2139–2152. doi: https://doi.org/10.3168/jds.2019-16787

Gilbert, Audrey, & Turgeon, S. L. (2021). Studying stirred yogurt microstructure and its correlation to physical properties: A review. *Food Hydrocolloids*, *121*, 106970. doi: https://doi.org/10.1016/j.foodhyd.2021.106970

Heck, A., Nöbel, S., Hitzmann, B., & Hinrichs, J. (2021). Volume Fraction Measurement of Soft (Dairy) Microgels by Standard Addition and Static Light Scattering. *Food Biophysics*, *16*(2), 237–253. doi: https://doi.org/10.1007/s11483-021-09665-z

Hyun, K., Wilhelm, M., Klein, C. O., Cho, K. S., Nam, J. G., Ahn, K. H., Lee, S. J., Ewoldt, R. H., & McKinley, G. H. (2011). A review of nonlinear oscillatory shear tests: Analysis and application of large amplitude oscillatory shear (LAOS). *Progress in Polymer Science*, *36*(12), 1697–1753. doi: https://doi.org/10.1016/j.progpolymsci.2011.02.002

Iijima, M., Hatakeyama, T., & Hatakeyama, H. (2021). DSC and TMA Studies of Polysaccharide Physical Hydrogels. *Analytical Sciences*, *37*(1), 211–219. doi: https://doi.org/10.2116/analsci.20SAR10

Le, A. N. M., Erturk, M. Y., Shim, Y. H., Rogers, S. A., & Kokini, J. (2023). A critical study of the nonlinear rheological properties in major classes of foods using the Sequence of Physical Processes (SPP) method and the Fourier Transform Coupled with Chebyshev Decomposition (FTC) method. *Food Research International*, *174*, 113587. doi: https://doi.org/10.1016/j.foodres.2023.113587

Li, Q., Xu, M., Xie, J., Su, E., Wan, Z., Sagis, L. M. C., & Yang, X. (2021). Large amplitude oscillatory shear (LAOS) for nonlinear rheological behavior of heterogeneous emulsion gels made from natural supramolecular gelators. *Food Research International*, *140*, 110076. doi: https://doi.org/10.1016/j.foodres.2020.110076

Martínez-Padilla, L. P. (2024). Rheology of liquid foods under shear flow conditions: Recently used models. *Journal of Texture Studies*, *55*(1). doi: https://doi.org/10.1111/jtxs.12802

McClements, D. J. (2023). Modeling the rheological properties of plant-based foods: Soft matter physics principles. *Sustainable Food Proteins*, *1*(3), 101–132. doi: https://doi.org/10.1002/sfp2.1015

Moussier, M., Guénard-Lampron, V., Lachin, K., Moulin, G., Turgeon, S. L., Michon, C., Huc-Mathis, D., & Bosc, V. (2019). What do stirred yogurt microgels look like? Comparison of laser diffraction, 2D dynamic image analysis and 3D reconstruction. *Food Structure*, *20*, 100107. doi: https://doi.org/10.1016/j.foostr.2019.100107

Najgebauer-Lejko, D., Witek, M., Żmudziński, D., & Ptaszek, A. (2020). Changes in the viscosity, textural properties, and water status in yogurt gel upon supplementation with green and Pu-erh teas. *Journal of Dairy Science*, *103*(12), 11039–11049. doi: https://doi.org/10.3168/jds.2020-19032

Ortíz-Deleón, A. M., Ramírez-Santiago, C., Sandoval-Castilla, O., Román-Guerrero, A., & Aguirre-Mandujano, E. (2023). Evaluation of physicochemical, rheological, textural and thermal properties of Mexican manchego-type cheese manufactured from goat s milk. *Revista Mexicana de Ingeniería Química*, *22*(1), 1–23. doi: https://doi.org/10.24275/rmiq/Alim3012

Ptaszek, P. (2017). Chapter 5 - Large Amplitude Oscillatory Shear (LAOS) Measurement and Fourier-Transform Rheology: Application to Food. In J. Ahmed, P. Ptaszek, & S. Basu (Eds.), Advances in Food Rheology and Its Applications (pp. 87–123). Woodhead Publishing, Elsevier. doi: https://doi.org/10.1016/B978-0-08-100431-9.00005-X

Rodríguez-Rodríguez, R., Espinosa-Andrews, H., Morales-Hernández, N., Lobato-Calleros, C., & Vernon-Carter, E. J. (2019). Mesquite gum/chitosan insoluble complexes: relationship between the water state and viscoelastic properties. *Journal of Dispersion Science and Technology*, *40*(9), 1345–1352. doi: https://doi.org/10.1080/01932691.2018.1513848

Rogers, S. (2018). Large amplitude oscillatory shear: Simple to describe, hard to interpret. *Physics Today*, *71*(7), 34–40. doi: https://doi.org/10.1063/PT.3.3971

Sala, G., de Wijk, R. A., van de Velde, F., & van Aken, G. A. (2008). Matrix properties affect the sensory perception of emulsion-filled gels. *Food Hydrocolloids*, *22*(3), 353–363. doi: https://doi.org/10.1016/j.foodhyd.2006.12.009

Sandoval-Castilla, O., Lobato-Calleros, C., Aguirre-Mandujano, E., & Vernon-Carter, E. J. (2004). Microstructure and texture of yogurt as influenced by fat replacers. *International Dairy Journal*, *14*(2), 151–159. doi: https://doi.org/10.1016/S0958-6946(03)00166-3

Suwannasang, S., Zhong, Q., Thumthanaruk, B., Vatanyoopaisarn, S., Uttapap, D., Puttanlek, C., & Rungsardthong, V. (2022). Physicochemical properties of yogurt fortified with microencapsulated Sacha Inchi oil. *LWT*, *161*, 113375. doi: https://doi.org/10.1016/j.lwt.2022.113375

Vélez-Ruiz, J. F., Barbosa Cánovas, G. V, & Peleg, M. (1997). Rheological properties of selected dairy products. *Critical Reviews in Food Science and Nutrition*, *37*(4), 311–359. doi: https://doi.org/10.1080/10408399709527778